

International Journal of Vehicle Noise and Vibration

ISSN online: 1479-148X - ISSN print: 1479-1471

<https://www.inderscience.com/ijvny>

Computational analysis on flow induced stress and acoustic vibration in a proposed silencer design for a three-cylinder in-line four-stroke spark ignition engine

Sushovan Chatterjee, Priyantha Bandara

DOI: [10.1504/IJVNV.2023.10055216](https://doi.org/10.1504/IJVNV.2023.10055216)

Article History:

Received:	28 June 2022
Accepted:	02 January 2023
Published online:	10 April 2023

Computational analysis on flow induced stress and acoustic vibration in a proposed silencer design for a three-cylinder in-line four-stroke spark ignition engine

Sushovan Chatterjee*

Department of Mechanical Engineering,
Cooch Behar Government Engineering College,
Cooch Behar, West Bengal – 736170, India
Email: sushovan.chatterjee@cgec.org.in
Email: sushovan.chatterjee@gmail.com
*Corresponding author

Priyantha Bandara

Department of Mechanical Engineering,
Sri Lanka Institute of Information Technology,
New Kandy Road, Malabe, Sri Lanka
Email: priyanthabandara92@yahoo.com

Abstract: Computational analysis of flowing exhaust gases inside a non-perforated silencer chamber of a commercially available three-cylinder inline four-stroke spark-ignition engine and in a modified perforated design was conducted and their respective levels of performance were predicted. Study on the existing and proposed silencer designs was carried out by way of computational fluid dynamics (CFD) analysis, structural analysis and modal analysis. Modal analysis has been performed in order to compute up to six fundamental frequencies on the aforementioned structure for analysing the response spectra for obtaining the natural frequencies at different modes of excitation. A reduction of 23.8% and 23.6% in the maximum values of static pressure and total pressure, respectively, has been observed for the proposed perforated model against the existing non-perforated silencer. The maximum acoustic power level and the maximum surface acoustic power level were found to be 9.5% and 7.3% respectively, less for the proposed design.

Keywords: computational analysis; CFD analysis; structural analysis; modal analysis; perforated silencer; non-perforated silencer.

Reference to this paper should be made as follows: Chatterjee, S. and Bandara, P. (2023) 'Computational analysis on flow induced stress and acoustic vibration in a proposed silencer design for a three-cylinder in-line four-stroke spark ignition engine', *Int. J. Vehicle Noise and Vibration*, Vol. 19, Nos. 1/2, pp.98–116.

Biographical notes: Sushovan Chatterjee is currently working as an Associate Professor and the Head of the Department of Mechanical Engineering, Cooch Behar Government Engineering College, under the Department of Higher Education, Government of West Bengal, India since December 2016. He is significantly involved in active interdisciplinary research in a versatile domain.

Priyantha Bandara is currently serving as a Senior Lecturer attached to the Department of Mechanical Engineering, Sri Lanka Institute of Information Technology. His research interests include computational fluid dynamics, building energy modelling and engineering education.

1 Introduction

In the present scenario, noise pollution has become one of the major environmental impacts (Gilani and Mir, 2021; Balasbaneh et al., 2020; Thakre et al., 2020). Increase in the number of automobiles necessitates the need to minimise the noise producing exhaust gas emissions from internal combustion (IC) engines (Qatu et al., 2009; Qatu, 2012). The exhaust gases possessing high pressure and temperature are allowed to pass through a silencer to attenuate the noise level (Munjal, 1998). There exist many types of mufflers such as baffle type, wave cancellation type, resonance type and absorptive type that operate by using their respective noise cancellation principles in order to achieve the purpose of the silencer (Balamurugan et al., 2015). Many studies in the field of muffler design can be found in the recent literature (Kalita and Singh, 2021; Kashikar et al., 2021; Mohamad et al., 2021; Kumar et al., 2022; Nag et al., 2022). Chatterjee (2016) reported a case study based on computational fluid dynamics approach for certain proposed designs of both absorptive as well as reactive type mufflers in which distribution of pressure, velocity and turbulent intensities of the flowing fluid inside the silencer were predicted. Na et al. (2014) simulated scattering of acoustic plane waves at sudden expansions for a three-dimensional duct having a rectangular cross-section with an expanding area using a linearised Navier-Stokes equation solver in the frequency domain. Shah et al. (2010) developed a model while working on a novel design of an automobile muffler and the analysis was carried out using modern Computer Aided Engineering (CAE) tools. Effective noise attenuation for a perforated muffler was validated by Parlar et al. (2013). Yu and Zhang (2013) proposed a mathematical model for simplifying the problem of radiation of sound power by a planar structure kept in a baffle. Lima et al. (2011) conducted a parametric optimisation study for reactive silencers using a genetic algorithm (GA). Wang et al. (2009) established the use of absorptive material for the reduction of transmission losses at resonant frequencies using boundary element method (BEM), finite element analysis (FEA) and experimental measurements. Wang (2023) further conducted an iterative hybrid analytical approach using both boundary element modelling as well as finite element modelling to find out the effect of cross members on sound transmission loss in an automotive floor panel where one dimensional acoustic space was considered in the structure surface inside the cross members. Liu et al. (2014) studied a plate silencer comprising an expansion chamber with two-sided branch rigid cavities covered by plates by calculating sound radiation in the duct and cavity and vibration velocity of the plate. Cui and Ji (2012) gave an insight on new techniques related to a silencer with fast multiple boundary element method (FMBEM). Jiang et al. (2010) divided a large silencer into physical modular units for analysis through the impedance matrix synthesis. Nazirkar et al. (2014) performed design and optimisation of an automotive muffler by incorporating changes such as avoiding natural frequency and use of a double expansion chamber. Munjal and Vijayasree (2012) presented an integrated transfer matrix method for the analysis of complex mufflers having multiple connecting parts and acoustic

elements by taking convective and dissipative effects of mean flow into account. Baruah and Chatterjee (2018) studied the structural deformation effects of perforation on an elliptical chamber muffler for a 4-stroke, 2-cylinder engine and also computational fluid dynamics (CFD) simulations of the exhaust gases through a typical muffler model (Baruah and Chatterjee, 2019). Caradonna (2011) performed a Computational Aero-Acoustic (CAA) modelling of simple as well as complex exhaust systems, integrated with conventional CFD and observed that the noise level was strongest at the outer-peripheral region due to the presence of a large pressure fluctuation. Chang et al. (2018) performed a numerical assessment of automotive mufflers using FEM, neural networks, by using a genetic algorithm. Chatterjee (2021) proposed four alternative design modifications for the geometrical configuration of the resonating chamber of a practical muffler, based on acoustic performance and reduction of back pressure through a simulation-based approach. Hou et al. (2022) suggested a modified corrugated perforated pipe design to replace the straight-through perforated pipe muffler for better noise attenuation. They analysed the influences of various structural parameters (such as perforation diameter, peak height, distance between adjacent peaks, and peak width) based on the transmission loss using multiple linear regression analysis.

Present work focuses on the analysis of flowing hot exhaust gases inside a silencer chamber of a commercially available three-cylinder inline four-stroke spark-ignition engine (Maruti OMNI) through the CFD approach. Structural (FEM-based strain and deformation subject to constraint conditions) and modal analyses (up to six fundamental frequencies) are also carried out for the perforated and non-perforated silencer and the results are validated in view of future practical application. Vibration analysis is carried out for studying the fatigue and thermal failure as well as to obtain the points of mounting on the basis of maximum strain deformation.

2 Governing principles

Certain theoretical aspects related to the present analysis are briefly discussed here.

2.1 Computational fluid dynamics

In the computational fluid dynamics (CFD) approach, numerical methodologies have been applied for solving Navier-Stokes equations that govern fluid flow and energy transfer. They are derived by applying conservation laws of mass (continuity), momentum, and energy to a fluid control volume. The said equations take the nonlinear partial differential form as shown in equation (1) (Tu et al., 2018):

$$\frac{\partial \phi}{\partial t} + (V \cdot \nabla)\phi - \Gamma_{\phi} \nabla^2 \phi = S_{\phi} \quad (1)$$

Moreover, governing equations on turbulence, combustion, species transport, etc. may be incorporated as per nature of the problem being handled. The computational domain is divided into non-overlapping control volumes generating a computational mesh. The size, shape and resolution of control volumes may influence the level of convergence, computational effort and accuracy of the CFD solution. The CFD solution is generated by solving the governing equations on the computational mesh by conducting simulations

until the state of convergence is reached. On reaching the state of convergence, CFD solution can be visualised or may be utilised for other post-processing tasks.

2.2 Modelling turbulence

Turbulent flows are found in many real engineering systems. Several approaches having different levels of complexity and computational intensity are applied in modelling turbulence. The main approaches include: direct numerical simulation (DNS), large eddy simulation (LES) and Reynolds-averaged Navier-Stokes (RANS) approach (Tu et al., 2018). DNS possesses the highest accuracy among the approaches mentioned above. However, the computational demand for this approach is very high. LES is the most preferred approach for flows with high Reynolds numbers or when the geometry is too complex for the DNS approach to be applied (Tu et al., 2018). For most engineering problems, influence of turbulence in terms of mean flow parameters is generally sufficient to quantify the turbulent flow characteristics (Tu et al., 2018). The RANS approach solves statistically-averaged Navier-Stokes equations using turbulent transport models. The standard k-ε model (Launder and Spalding, 1974) is the most widely used and validated turbulence model that can handle a variety of engineering flow problems (Tu et al., 2018). It is a two-equation model representing turbulent kinetic energy (k) and the rate of dissipation of turbulent energy (ϵ) as shown in equations (2) and (3) (Versteeg and Malalasekera, 1995).

$$l = \frac{k^{\frac{3}{2}}}{\epsilon} \tag{2}$$

where l is the length scale

$$\mu_t = \rho C_\mu \frac{k^2}{\epsilon} \tag{3}$$

where μ_t is the turbulent viscosity and C_μ is a dimensionless constant.

2.3 Structural analysis

General three-dimensional stress is calculated in terms of three normal and three shear stress components aligned to the part or assembly coordinate system. The principal stresses and the maximum shear stress are called invariants, that is, their values do not depend on the orientation of the part or assembly with respect to its world coordinates system. The principal strains ϵ_1 , ϵ_2 and ϵ_3 as well as the maximum shear strain Y_{\max} can also be calculated. The principal strains have the relationship $\epsilon_1 > \epsilon_2 > \epsilon_3$.

Equivalent stress (von Mises) is related to the principal stresses as given in equation (4):

$$\sigma_B = \left[\frac{(\sigma_1 - \sigma_2)^2 + (\sigma_2 - \sigma_3)^2 + (\sigma_3 - \sigma_1)^2}{2} \right]^{\frac{1}{2}} \tag{4}$$

The von Mises or equivalent strain ϵ_e is computed as shown in equation (5):

$$\varepsilon_e = \frac{1}{1+\nu} \left[\frac{(\varepsilon_1 - \varepsilon_2)^2 + (\varepsilon_2 - \varepsilon_3)^2 + (\varepsilon_3 - \varepsilon_1)^2}{2} \right]^{\frac{1}{2}} \quad (5)$$

2.4 Modal analysis

A system is characterised by different modes of vibration where each mode has a modal frequency and a mode shape. Aim of this analysis is to find the natural frequencies of vibration for different modes and to check whether any of these frequencies matches with the working frequency range of the system. This analysis helps in checking the occurrence of resonance in the muffler and for selection of mounting points in the zone of maximum strain deformation. The muffler is considered to be a 6-degrees of freedom (DOF) body system as the free vibrations are prominent in the first few harmonics.

2.5 Acoustic fluid structure interaction

In acoustic fluid structure interaction problems, the structural dynamics equation can be formulated using the structural elements, fluid momentum and continuity equation and through equations that are simplified to obtain the acoustic wave equation.

The acoustic wave equation is given by:

$$\frac{1}{c^2} \frac{\partial^2 P}{\partial t^2} - \nabla^2 P = 0 \quad (6)$$

where c is the speed of sound ($\sqrt{K/\rho_0}$) in the fluid medium. ρ_0 , K , P and t are mean fluid density, bulk modulus of the fluid, acoustic pressure and time, respectively.

For the propagation of sound in the fluids, viscous dissipation may be neglected that is related to the losses wave equation. In that case, discretised structure equation and the losses wave equation (6) have to be considered simultaneously in fluid-structure integration problems (Everstine, 1997; Greenshields and Weller, 2005; He, 2020; Gorakifard et al., 2021).

3 Design and modelling

Present work deals with design modifications carried out to an existing silencer model through computational modelling and analysis. Dimensions of the geometrical model of the three-cylinder inline SI engine have been taken from an existing commercial silencer model of a four-wheeler. The technical specifications of the engine and the existing silencer model are shown in Tables 1a and 1b, respectively.

Table 1a Engine specifications

<i>Parameter</i>	<i>Value</i>
Type of engine	3-cylinder in-line 4-stroke S.I. engine
Engine speed	5,000 rpm
Maximum engine frequency	83.33 Hz
Working frequency range	7.30–83.33 Hz

Table 1b Specifications of the existing silencer

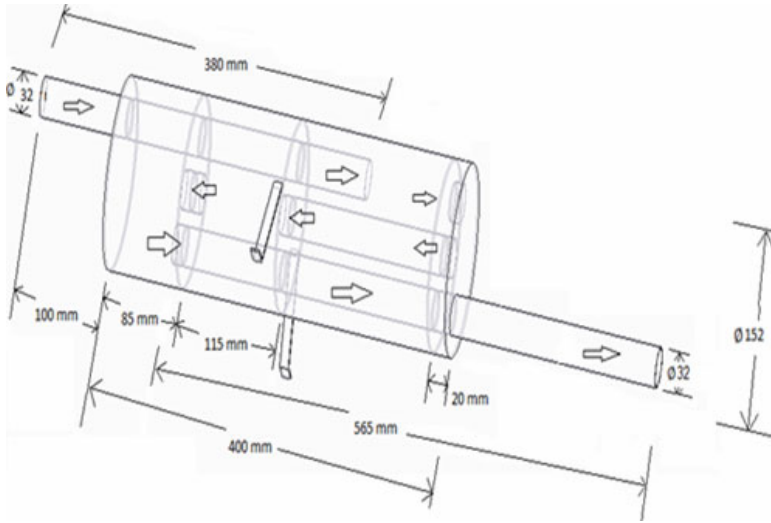
<i>Parameter</i>	<i>Value</i>
Type of muffler	Reactive type (offset inlet and outlet pipes)
Type of resonating chamber	Multiple (3 nos. of chambers)
Cross-section of resonating chamber	Circular
Perforations	None
Baffles	None
Diameter of the resonating chamber	152 mm
Total length of the resonating chamber	400 mm
External diameter of the inlet pipe	32 mm
Internal diameter of the inlet pipe	30 mm
Total length of inlet pipe	380 mm
Total length of outlet pipe	565 mm

Table 2 shows flow physics and boundary conditions applied during computational simulations.

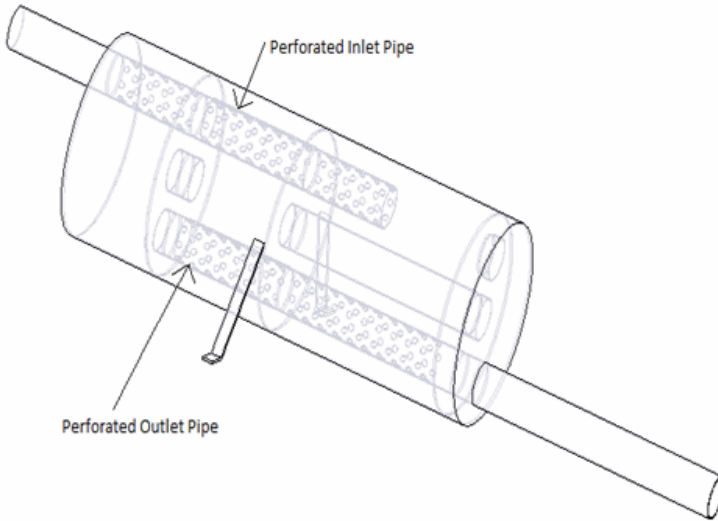
Table 2 Flow physics and boundary conditions

<i>Flow physics/boundary conditions</i>	<i>Parameter/model</i>	<i>Value</i>
Material properties	Density	7,850 kg/m ³
	Thermal expansion coefficient	1.2×10 ⁻⁵ K ⁻¹
	Specific heat capacity	460 J/kgK
	Thermal conductivity	6.05×10 ⁻² W/mm/K
	Compressive yield strength	250 MPa
	Ultimate tensile strength	460 MPa
	Poisson's ratio	0.3
	Bulk modulus	1.67×10 ⁵ MPa
	Shear modulus	76,923 MPa
Fluid properties	Density	1.225 kg/m ³
	Specific heat at constant pressure	1,006.43 J/kgK
	Thermal conductivity	0.0242 W/mK
	Viscosity	1.7894×10 ⁻⁵ kg/ms
Models/boundary conditions	Turbulence modelling	RANS approach with standard k-ε turbulence model
	Inlet temperature of air	828 K
	Inlet pressure of air	276 kPa
	Inlet velocity of air	116 m/s
	Outlet temperature of air	343 K

Figure 1 Muffler models, (a) non-perforated silencer (existing model) (b) perforated silencer (proposed modified model)



(a)



(b)

Figure 1 shows the configurations of the exiting non-perforated silencer model [Figure 1(a)] and the proposed modified muffler model [Figure 1(b)]. No perforation is present in the exiting model, whereas in the proposed model, perforations have been provided in both inlet and exhaust pipes. Perforation is provided in order to facilitate expansion of the exhaust gases. This saves material and makes the silencer light weight.

4 Results and discussion

The results have been presented in the paper under three analyses, the first of which includes CFD analysis in terms of contour plots of static and total pressure, velocity, turbulent intensity, acoustic power level and surface acoustic power level. Second analysis covers structural analysis for stress and strain deformation, and the third gives an insight of the performance of the system based on modal analysis.

4.1 CFD analysis

Due to pressure and density fluctuations, sound waves emitted from an exhaust system possess different frequencies. Attenuation of the said undesirable frequencies is the role of the silencer or muffler. The total pressure of exhaust gases has primarily two components viz. static and dynamic pressure. Static pressure is usually measured by a device moving with the flow whereas dynamic pressure is associated with the velocity of flow. This is where the CFD analysis holds significant. In this context, total pressure is determined as the sum of static and dynamic pressure. CFD results in this regard are shown in Table 3.

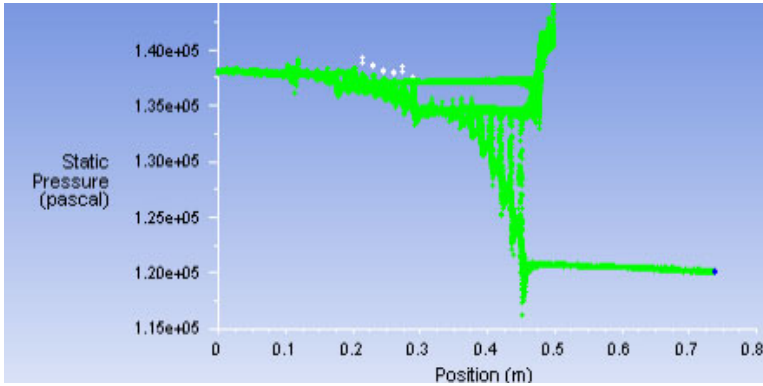
Table 3 CFD simulation results

<i>Parameter</i>	<i>Perforated model</i>		<i>Non-perforated model (existing model)</i>	
	<i>Maximum</i>	<i>Minimum</i>	<i>Maximum</i>	<i>Minimum</i>
Static pressure (Nm ⁻²)	1.44×10 ⁵	1.16×10 ⁵	1.89×10 ⁵	1.10×10 ⁵
Total pressure (Nm ⁻²)	1.46×10 ⁵	1.20×10 ⁵	1.91×10 ⁵	1.14×10 ⁵
Velocity (m/s)	156.8	0	218.6	0
Turbulent intensity (%)	19.50	0.41	33.60	0.46
Acoustic power level (dB)	134	0	148	0
Surface acoustic power level (dB)	126	0	136	0

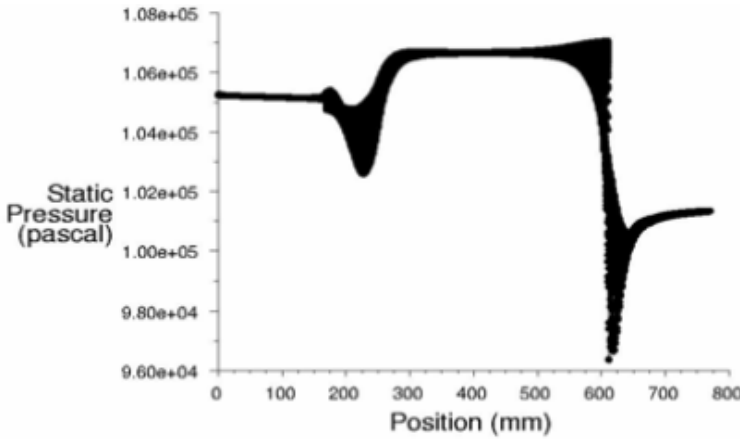
4.1.1 Static pressure

Figure 2(a) illustrates the static pressure profile in the proposed model (perforated). The static pressure profile predicted by CFD during present work is found similar to the work done by Mohiuddin et al. (2007) as shown in Figure 2(b). In both cases, the fluctuation of static pressure shows similar trends. Owing to the stack-up or stagnation of the flowing gas inside the expansion chamber, there was an escalation in static pressure because of the cross-sectional variation between resonating chamber and the outlet. There is a marginal increment of the exhaust velocity as this high pressure forcefully drives out the exhaust gas to the ambient environment. This pressure drop causes the velocity to increase.

Figure 2 Static pressure distribution, (a) static pressure profile of perforated design model (b) Static pressure profile of Mohiuddin et al. (2007) (see online version for colours)



(a)



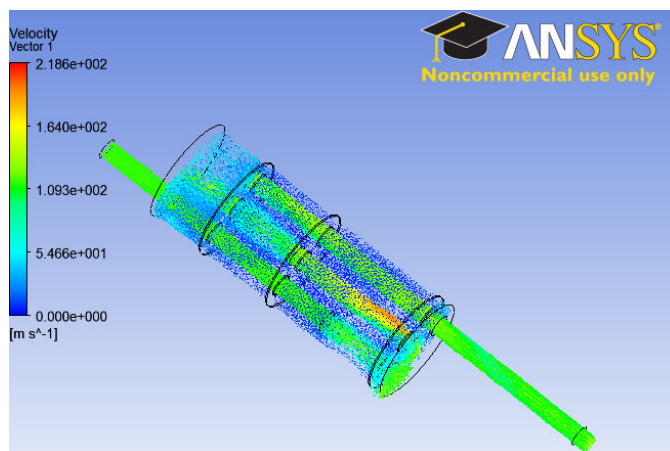
(b)

4.1.2 Velocity distribution

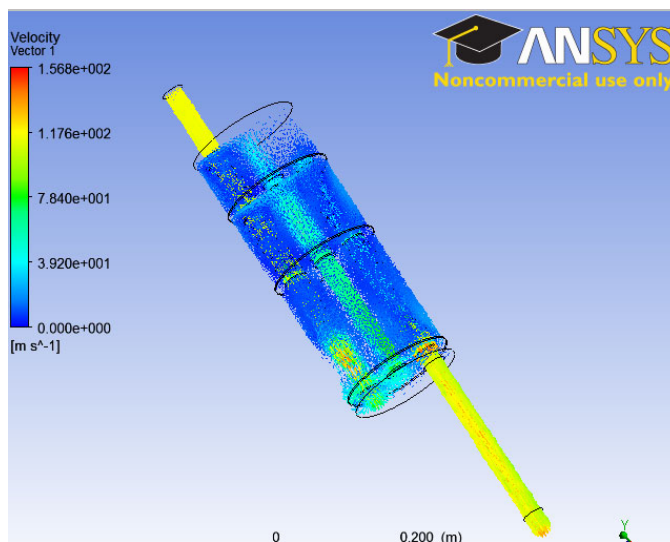
The velocity flow field for the existing as well as the proposed model is shown in Figure 3. CFD analysis predicted a maximum exhaust gas velocity of 156.8 m/s and 218.6 m/s for the perforated and non-perforated models respectively. Caradonna (2011) also found similar trends as obtained from the present analysis. There is a considerable reduction in velocity in the proposed perforated silencer than that of the existing one. This corresponds to a substantial reduction in the noise level as well.

It is observed that in the perforated silencer, release of exhaust gas pressure is well facilitated which produces a less pressure distribution throughout the silencer. A substantial reduction in velocity, acoustic power and acoustic surface power have been observed in the perforated silencer that leads to a considerable reduction in the noise level.

Figure 3 Velocity flow field (a) existing model (non-perforated) (b) proposed model (perforated) (see online version for colours)



(a)

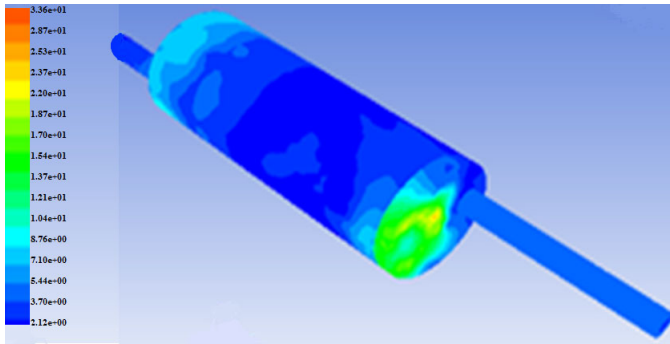


(b)

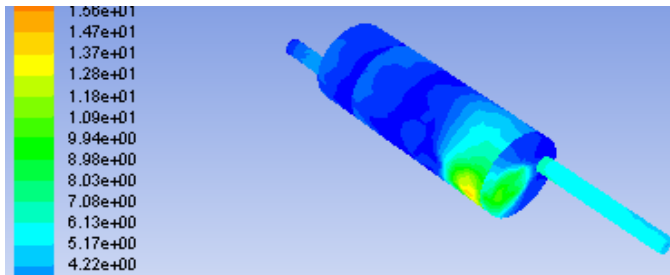
4.1.3 Turbulent intensity

The turbulent intensities of the existing model and the proposed perforated model are shown in Figure 4. It is observed that the maximum turbulent intensity has reduced by a substantial value (42%) in the proposed design.

Figure 4 Turbulent intensity (%), (a) existing model (non-perforated) (b) proposed model (perforated) (see online version for colours)



(a)

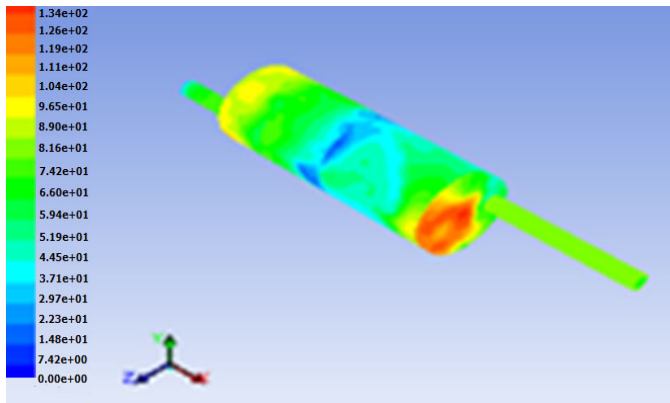


(b)

4.1.4 Acoustic power and Surface acoustic power level

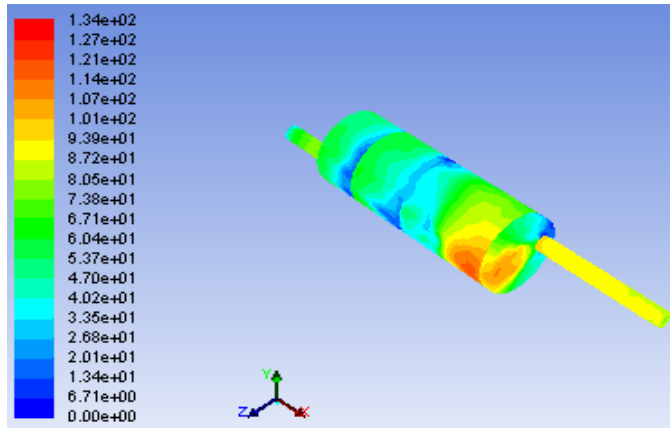
The acoustic power level and surface acoustic power level have also been found to be reduced by 9.5% and 7.3% respectively, in the proposed design. The relevant contours are shown in Figures 5 and 6 respectively.

Figure 5 Acoustic power level (dB), (a) existing model (non-perforated) (b) proposed model (perforated) (see online version for colours)



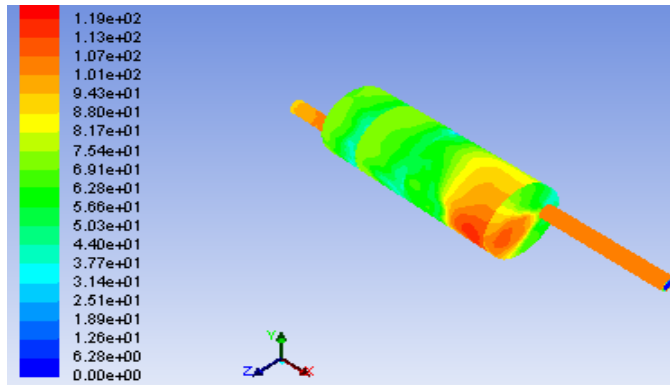
(a)

Figure 5 Acoustic power level (dB), (a) existing model (non-perforated) (b) proposed model (perforated) (continued) (see online version for colours)

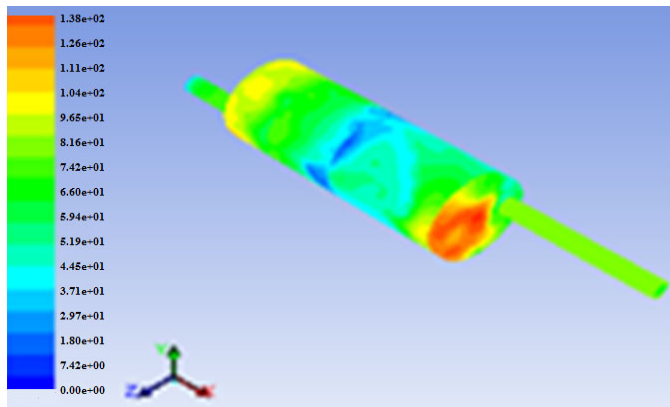


(b)

Figure 6 Surface acoustic power level (dB), (a) existing model (non-perforated) (b) proposed model (perforated) (see online version for colours)



(a)



(b)

4.2 Structural analysis

In order to perform structural analysis, pressure and temperature fields generated by the CFD analysis were imported to the structural module of ANSYS 14.0 workbench. The structural analysis results are shown in Table 4. It is observed that the perforated silencer is subjected to higher stress, strain and total deformation when compared with that of the non-perforated silencer. This is due to possible decrease in overall strength as a result of the presence of perforations in the silencer. However, this effect is negligible as far as the benefits gained through noise reduction are concerned.

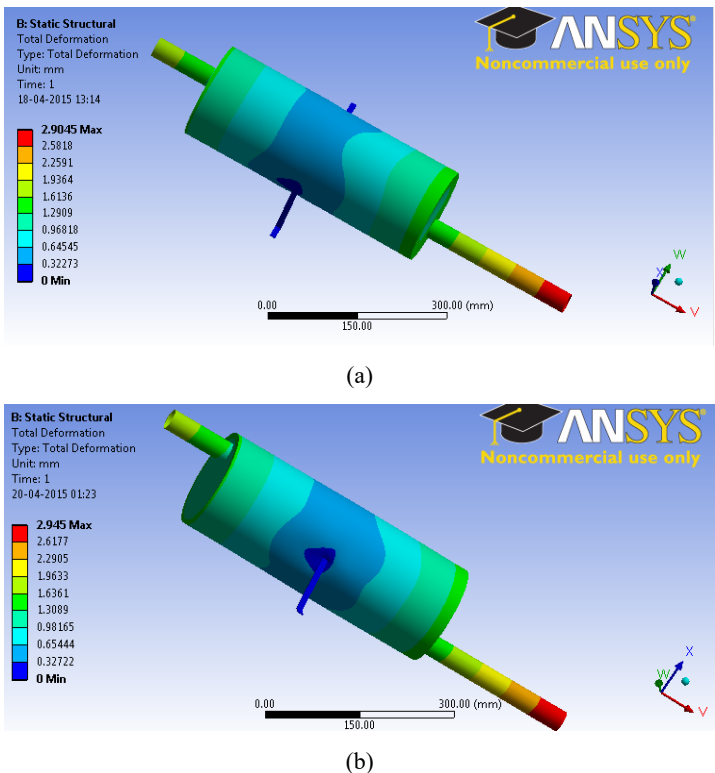
Table 4 Results of structural analysis

Parameters	Non-perforated model	Perforated model
Total deformation (mm)	2.904	2.945
Equivalent strain (mm/mm)	0.029	0.033
Equivalent (Von-Mises) stress (MPa)	4,645.2	5,221.3

4.2.1 Deformation behaviour

It is evident from Figure 7 that the maximum total deformation was found to be 1.4% higher for the perforated model when compared against the existing model.

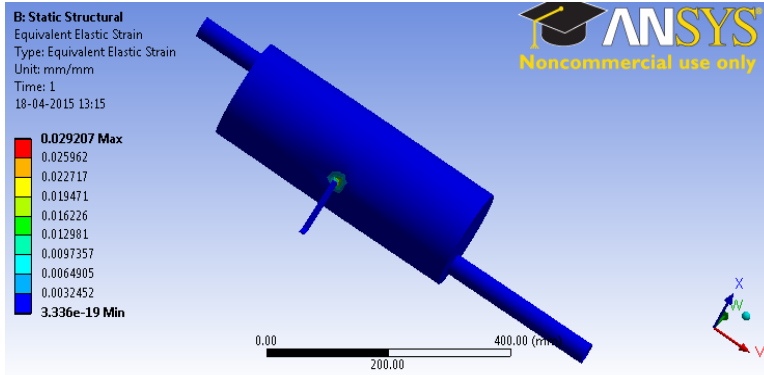
Figure 7 Static deformation, (a) existing model (non-perforated) (b) proposed model (perforated) (see online version for colours)



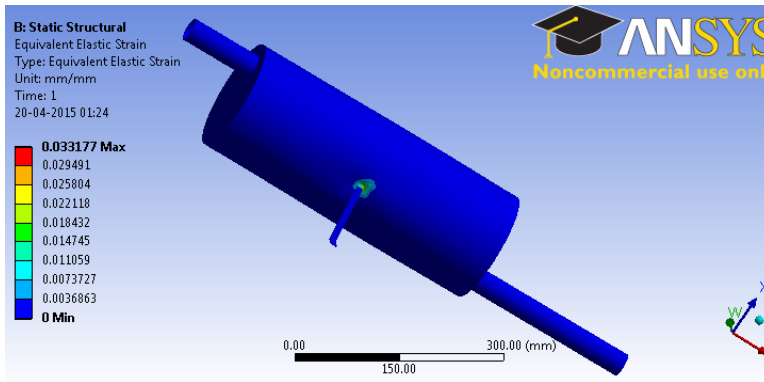
4.2.2 Equivalent strain

As per Figure 8, equivalent elastic strain is found to be 13.8% higher for the perforated model when compared against the existing model.

Figure 8 Equivalent strain, (a) existing model (non-perforated) (b) proposed model (perforated) (see online version for colours)



(a)



(b)

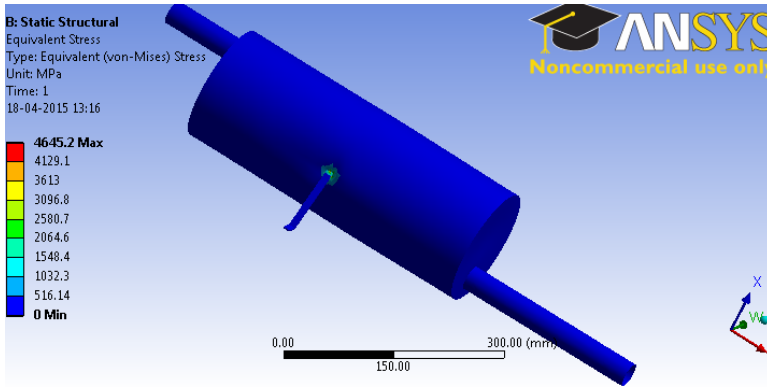
4.2.3 Von Mises stress

According to Figure 9, von Mises stress was reported to be 12.4% higher in the perforated model when compared against the existing model.

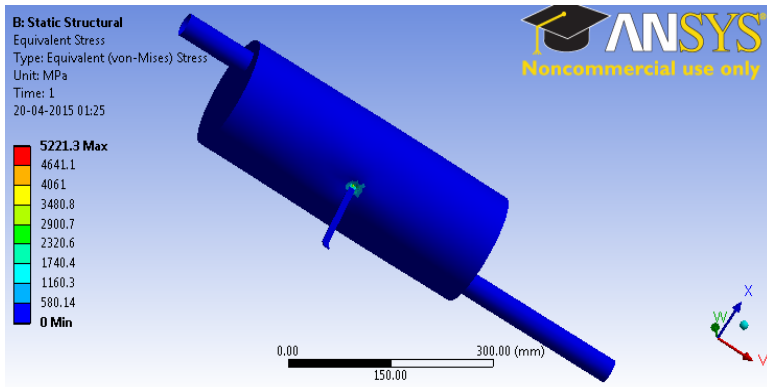
4.3 Modal Analysis

The main objective of the modal analysis is to determine natural modes and natural frequencies during free vibration. The results so obtained are then calibrated with those obtained from FEM analysis to justify the material properties and boundary conditions. The results of modal analysis are summarised in Table 5.

Figure 9 Equivalent (von Mises) stress, (a) existing model (non-perforated) (b) proposed model (perforated) (see online version for colours)



(a)

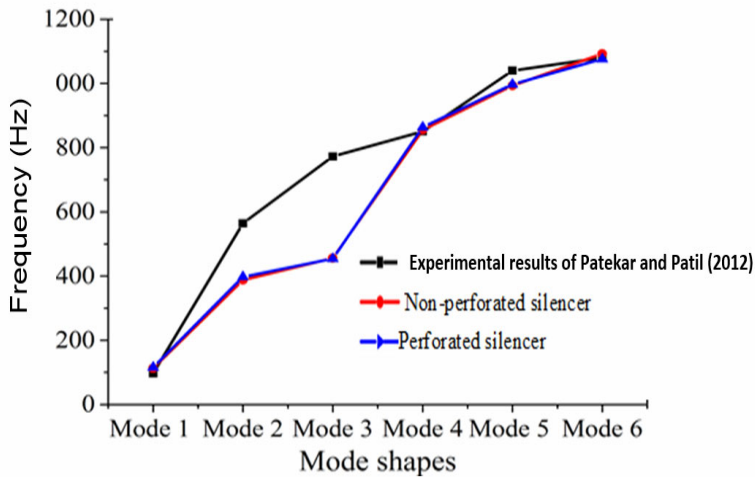


(b)

Table 5 Modal analysis

Mode shape	Frequency (Hz)	
	Perforated model	Non-perforated model
Mode shape 1	115.94	113.01
Mode shape 2	397.25	387.85
Mode shape 3	454.23	455.59
Mode shape 4	863.45	855.33
Mode shape 5	997.24	993.22
Mode shape 6	1,076.00	1,092.00

Similar modal trends have been observed in experimental work conducted by Patekar and Patil (2012). The comparison among the said experimental observations and computational predictions for mode shapes at six natural frequencies are shown in Figure 10.

Figure 10 Modal frequencies (see online version for colours)

5 Conclusions

It is observed that reductions of 23.8% and 23.6% are reported with respect to the maximum values of static pressure and total pressure respectively, for the proposed perforated model of the silencer against the existing non-perforated design. Furthermore, maximum velocity was also found to be 28.3% lower in case of the proposed model. Moreover, the maximum turbulent intensity was reduced by a margin of 42%. The maximum acoustic power and maximum surface acoustic power were also found to be 9.5% and 7.3% respectively, less in the proposed design.

As opposed to the above, total deformation, equivalent elastic strain and von Mises stress have increased by 1.4%, 13.8% and 12.4% respectively for the perforated model when compared against the existing model. This may be due to weakening of the overall strength of the silencer due to the presence of perforations. However, this drawback is considered to be negligible as far as the benefits gained due to enhanced noise attenuation capability of the perforated silencer are concerned.

Acknowledgements

The authors are thankful for the support extended by Mr. Rajesh Kumar Meena in conducting computational simulations.

References

- Balamurugan, S., Jeyaprakash, N. and Manikandan, K. (2015) 'Design and fabrication of muffler for four stroke diesel engine', *International Journal of Scientific Engineering and Technology*, Vol. 3, No. 4, pp.136–140.
- Balasanbhan, A.T., Yeoh, D. and Abidin, A.R.Z. (2020) 'Life cycle sustainability assessment of window renovations in schools against noise pollution in tropical climates', *Journal of Building Engineering*, Vol. 32, p.101784.
- Baruah, S. and Chatterjee, S. (2019) 'CFD analysis on an elliptical chamber muffler of a C.I. engine', *International Journal of Heat and Technology*, Vol. 37, No. 2, pp.613–619.
- Baruah, S. and Chatterjee, S. (2018) 'Structural analysis for exhaust gas flow through an elliptical chamber muffler under static and dynamic loading condition', *Advances in Modelling and Analysis B*, Vol. 61, No. 2, pp.92–98.
- Caradonna, J. (2011) 'Advanced computational aero-acoustic simulation of complex automotive exhaust systems', *SAE International Journal of Materials and Manufacturing*, Vol. 4, No. 1, pp.685–695.
- Chang, Y.C., Chiu, M-C. and Wu, M-R. (2018) 'Numerical assessment of automotive mufflers using FEM, neural networks, and a genetic algorithm', *Archives of Acoustics*, Vol. 43, No. 3, pp.517-529.
- Chatterjee, S (2021) 'Acoustic performance and modal analysis for the muffler of a four-stroke three-cylinder inline spark ignition engine', *International Journal of Simulation and Process Modelling*, Vol. 16, No. 3, pp.247–255.
- Chatterjee, S. (2016) 'Computational fluid dynamic analysis of the exhaust gas flow through absorptive and reactive mufflers: some case studies', *Proceedings of the IMechE, Part D: Journal of Automobile Engineering*, Vol. 231, No. 11, pp.1568–1588.
- Cui, X.B. and Ji, Z.L. (2012) 'Fast multi pole boundary element approaches for acoustic attenuation prediction of reactive silencers', *Engineering Analysis with Boundary Elements*, Vol. 36, No. 7, pp.1053–1061.
- Everstine, G.C. (1997) 'Finite element formulations of structural acoustics problems', *Computers & Structures*, Vol. 65, No.3, pp.307–321.
- Gilani, T.A. and Mir, M.S. (2021) 'A study on the assessment of traffic noise induced annoyance and awareness levels about the potential health effects among residents living around a noise-sensitive area', *Environmental Science and Pollution Research*, Vol. 28, No. 44, pp.1–20.
- Gorakifard, M., Cuesta, I., Saluena, C. and Far, E.K. (2021) 'Acoustic wave propagation and its application to fluid structure interaction using the cumulant lattice Boltzmann method', *Computers & Mathematics with Applications*, Vol. 87, pp.91–106.
- Greenshields, C.J. and Weller, H.G. (2005) 'A unified formulation for continuum mechanics applied to fluid-structure interaction in flexible tubes', *International Journal for Numerical Methods in Engineering*, Vol. 64, No. 12, pp.1575–1593.
- He, T. (2020) 'A strongly-coupled cell-based smoothed finite element solver for unsteady viscoelastic fluid-structure interaction', *Computers & Structures*, Vol. 235, p.106264.
- Hou, Z., Xu, T., Zhang, Z. and Sun, J. (2022) 'Case study: numerical study of the noise reduction characteristics of corrugated perforated pipe mufflers', *Noise Control Engineering Journal*, Vol. 70, No. 1, pp.16–36.
- Jiang, C., Wu, T.W. and Cheng, C.Y.R. (2010) 'A single-domain boundary element method for packed silencers with multiple bulk-reacting sound absorbing materials', *Engineering Analysis with Boundary Elements*, Vol. 34, No. 11, pp.971–976.
- Kalita, U. and Singh, M. (2021) 'Design and CFD analysis on flow through a reactive muffler of four-cylinder diesel engine', *Recent Trends in Engineering Design*, pp.211–223, Springer, Singapore.

- Kashikar, A., Suryawanshi, R., Sonone, N., Thorat, R. and Savant, S. (2021) 'Development of muffler design and its validation', *Applied Acoustics*, Vol. 180, p.108132.
- Kumar, R.R., Razak, A., Alshahrani, S., Sharma, A., Thakur, D., Shaik, S., Saleel, C.A. and Afzal, A. (2022) 'Vibration analysis of composite exhaust manifold for diesel engine using CFD', *Case Studies in Thermal Engineering*, Vol. 32, p.101853.
- Lauder, B. and Spalding, D. (1974) 'The numerical computation of turbulent flows', *Computer Methods in Applied Mechanics and Engineering*, Vol. 3, No. 2, pp.269–289.
- Lima, K.F.D., Lenzi, A. and Barbieri, R. (2011) 'The study of reactive silencers by shape and parametric optimization techniques', *Applied Acoustics*, Vol. 72, No. 4, pp.142–150.
- Liu, G., Zhao, X., Zhang, W. and Li, S. (2014) 'Study on plate silencer with general boundary conditions', *Journal of Sound and Vibration*, Vol. 333, No. 20, pp.4881–4896.
- Mohamad, B., Karoly, J., Zelentsov, A. and Amroune, S. (2021) 'A comparison between hybrid method technique and transfer matrix method for design optimization of vehicle muffler', *FME Transactions*, Vol. 49, No. 2, pp.494–500.
- Mohiuddin, A.K.M., Aatur, R. and Gazali, Y.B. (2007) 'Simulation and experimental investigation of muffler performance', *International Journal of Mechanical and Materials Engineering*, Vol. 2, No. 2, pp.118–124.
- Munjal, M.L. (1998) 'Analysis and design of muffler over view of research at the Indian Institute of Science', *Journal of Sound and Vibration*, Vol. 211, No. 3, pp.425–433.
- Munjal, M.L. and Vijayasree, N.K. (2012) 'On an integrated transfer matrix method for multiply connected mufflers', *Journal of Sound and Vibration*, Vol. 331, No. 8, pp.1926–1938.
- Na, W., Efraimsson, G. and Boij, S. (2014) 'Simulations of the scattering of sound waves at a sudden area expansion in a 3-D duct', *21st International Congress on Sound and Vibration*, Beijing, China, pp.1420–1427.
- Nag, S., Dhar, A., and Gupta, A. (2022) 'Automotive exhaust thermoelectric generator unit integrated to exhaust noise muffler: heat recovery and noise attenuation simulations', *Engine Modelling and Simulation*, pp.323–340, Springer, Singapore.
- Nazirkar, R.D., Meshram, S.R., Namdas, A.D., Navagire, S. and Devarshi, S.S. (2014) 'Design & optimization of exhaust muffler & design validation', *International Journal of Mechanical and Production Engineering*, Vol. 2, No. 10, pp.20–26.
- Parlar, Z., Ari, S., Yilmaz, R., Özdemir, E. and Kahraman, A. (2013) 'Acoustic and flow field analysis of a perforated muffler design', *Engineering and Technology*, Vol. 7, No. 3, pp.447–451.
- Patekar, V.P. and Patil, R.B. (2012) 'Vibrational analysis of automotive exhaust silencer based on FEM and FFT analyzer', *International Journal on Emerging Technologies*, Vol. 3, No. 2, pp.1–3.
- Qatu, M.S. (2012) 'Recent research on vehicle noise and vibration', *International Journal of Vehicle Noise and Vibration*, Vol. 8, No. 4, pp.289–301.
- Qatu, M.S., Abdelhamid, M.K., Pang, J. and Sheng, G. (2009) 'Overview of automotive noise and vibration', *International Journal of Vehicle Noise and Vibration*, Vol. 5, Nos. 1–2, pp.1–35.
- Shah, S., Saisankaranarayana, K., Hatti, K.S. and Thombare, D.G. (2010) *A Practical Approach towards Muffler Design, Development and Prototype Validation*, SAE Technical Paper 2010-32-0021.
- Thakre, C., Laxmi, V., Vijay, R., Killedar, D. J. and Kumar, R. (2020) 'Traffic noise prediction model of an Indian road: an increased scenario of vehicles and honking', *Environmental Science and Pollution Research International*, Vol. 27, No. 30, pp.38311–38320.
- Tu, J., Yeoh, G. H. and Liu, C. (2018) *Computational Fluid Dynamics: A Practical Approach*, 3rd ed., Butterworth-Heinemann, Cambridge, USA.
- Versteeg, H.K. and Malalasekera, W. (1995) *An Introduction to Computational Fluid Dynamics: The Finite Volume Method*, Longman, Harlow, England.

- Wang, C. (2023) 'Sound transmission loss of an automotive floor panel section with cross members', *Applied Acoustics*, Vol. 202, p.109177.
- Wang, C.N., Wu, C.H. and Wu, T.D. (2009) 'A network approach for analysis of silencers with/without absorbent material', *Applied Acoustics*, Vol. 70, No. 3, pp.208–214.
- Yu, D. and Zhang, J. (2013) 'A simplified formula for calculating the sound power radiated by planar structures', *International Journal of Acoustics and Vibration*, Vol. 18, No. 2, pp.91–93.